Modulation of Gulf Stream Surface–Subsurface Frontal Separation by Path Curvature

CHARLES W. HORTON

Naval Oceanographic Office, NSTL, Bay St. Louis, MS 39522

(Manuscript received 19 August 1985, in final form 9 October 1986)

ABSTRACT

Observations of surface–subsurface frontal separation have inconsistently demonstrated a relationship between surface–subsurface frontal separation and subsurface-front path curvature. An analytical model of surface–subsurface frontal separation shows that this separation is modulated by curvature of the path of the subsurface front, and that the strength of this modulation is approximately proportional to the surface–subsurface frontal separation. A comparison of the theory with observations shows agreement.

1. Introduction

A major difficulty with the remote sensing of oceanographic phenomena is inferring knowledge of the subsurface structure of the ocean from surface observations. For example, the surface front of the Gulf Stream can usually be sensed using satellite infrared imagery. However, inferring the path of the Stream beneath the mixed layer is not straightforward. Observers have consistently found the separation between the Stream's surface front and the path of the 15°C isotherm at 200 m, the common definition of the subsurface front, to be highly variable (Hansen and Maul, 1970; Robinson et al., 1974; Horton, 1984a,b). Fortunately, part of this variability in separation can be related to curvature in the Stream's path (Hansen and Maul, 1970). The observations of Horton (1984a), which will be examined here in more detail, support their conclusion. In contrast, later observations (Horton, 1984b) show no obvious evidence of a relationship between the path curvature and the surface–subsurface frontal separation. Our purpose here is to obtain a relationship between frontal separation and the path curvature of the Stream for the purpose of understanding why the dependence of surface–subsurface frontal separation upon path curvature is only intermittently seen.

2. Discussion

As is well known, the width of the stream tends to vary from trough to peak as the stream meanders. Observations shown by Fuglister and Worthington (1951), Chew (1974), and Newton (1978) among others illustrate this effect. The time series of Gulf Stream sections by Webster (1961) are relevant if the measurements are interpreted as a spatial series passing a point. Observations upstream of Cape Hatteras, such as by Bane et al. (1981) do not necessarily demonstrate a strong curvature effect. This is because the meander envelope and, hence the maximum path curvature of the Gulf Stream are restricted there. Finally, Rossby et al. (1985) is an excellent recent reference on the general subject.

As Newton (1978) discusses, the changing width of the stream during meandering arises from the changing centripital acceleration associated with the stream's curvature. Using natural coordinates to describe the Gulf Stream's cross-stream momentum balance, the terms balancing the cross-stream pressure gradient are $v(f + vK)$ where K is the Stream's path curvature and v is the horizontal current speed. Viewing the cross-stream momentum balance in this form it is readily apparent that the centripital accelerations can add or subtract to the Coriolis parameter. Where the Stream's flow is cyclonic the accelerations due to the Coriolis parameter and the curvature add leading to a narrower Stream with a steeper cross-stream slope of the subsurface fronts. Conversely, where the Stream's flow is anticyclonic the accelerations due the Corolis parameter and the curvature are of opposite sign leading to wider Stream with a smaller cross-stream slope of the subsurface front.

The derivation for the frontal separation will proceed in two steps. The first step employs an analytical model of stable meanders in the stream by Stommel (1972). The model used has two layers. The upper layer of depth h is a constant potential voriticity layer while the lower layer is at rest. The presence of the mixed layer is formally ignored. The position of the interface between the two layers at 200-m depth is the position of the subsurface front. Likewise, the location of the surface front is taken to be where the depth h vanishes. In this model the separation between the surface and subsurface fronts is the depth difference between the surface and subsurface fronts divided by the average cross-stream slope of the interface over that depth range. This is essentially what was done in a model by

Maul (1975) except that here we will assume that the Stream's potential vorticity is the same at meander troughs and peaks. Maul relaxed this assumption by requiring that current speeds where h was 200-m depth be the same at meander troughs and peaks.

While this model predicts that the frontal separation should be modulated by path curvature, it does not explain why the curvature effect is only intermittently seen. The problem with this derivation is that it assumes that the surface front (which is really the mixed-layer front) is where the subsurface front outcrops in the mixed-layer. This is in general not true. That is, the surface front need lie over the same isopycnal that the subsurface front is on as is demonstrated by the observed very variable surface–subsurface frontal separation. For this reason changes in the horizontal separations between the isopycnals forming the Gulf Stream's fronts need to be considered in addition to just the changes in the cross-stream slope of these isopycnals. This is done in the second part of the derivation.

3. Derivation

As did Stommel (1972), we assume a meridional current with downstream current speed v having small amplitude stable meanders. The current is confined to the upper layer which has depth h. The momentum balance describing the current is

$$fv+\frac{v^2}{R}=g'\frac{\partial h}{\partial x} \tag{1}$$

where

- f the Coriolis parameter
- g the acceleration of gravity
- g' $(=g\Delta\rho/\rho)$
- $\Delta\rho$ the density difference between the two layers
- x the coordinate to the right of the downstream flow direction
- R the radius of curvature defined such that R is positive for cyclonic curvature.

Additionally, if it is supposed that potential vorticity is conserved in the upper layer,

$$\frac{f+\partial v/\partial x}{h}=\frac{f}{h_0} \tag{2}$$

where h_0 is the value of h at $x \to \infty$.

Combining Eqs. (1) and (2) we obtain

$$v+\frac{v^2}{\alpha Rc}=\frac{1}{\alpha^2}\frac{\partial^2 v}{\partial x^2} \tag{3}$$

where $c=(g'h_0)^{1/2}$ and $\alpha=f/c$. The solution to equation 3 is

$$v=\frac{Ce^{-\alpha x}}{[1-(e^{-\alpha x}/6\alpha R)]^2}. \tag{4}$$

The solution for h is obtained by substituting the derivative of Eq. (4) into Eq. (2). Doing this gives

$$h=h_0\left[1-\frac{e^{-\alpha x}}{[1-(e^{-\alpha x}/6\alpha R)]^2}-\frac{e^{-2\alpha x}}{3\alpha R[1-(e^{-\alpha x}/6\alpha R)]^3}\right]. \tag{5}$$

Stommel (1972) solved Eq. (3) using a series solution which assumed αR to be much greater than one. By making the same assumption in order to express them in the form of a Taylor series, Eqs. (4) and (5) yield Stommel's series solutions.

Figure 1 plots h versus x using Eq. (5) for several different curvatures K where K is $1/R$. The case with cyclonic or positive curvatures shows a steeper slope $\partial h/\partial x$ than does the case with anticyclonic or negative curvature. Note that the depth h never vanishes for the case with the greatest anticyclonic curvature. For this case the minimum value of h is reached where vK, which is negative, becomes equal in magnitude to f. This is consequence of the unrealistically high velocities which the model predicts, in this case in excess of 4 m s^{-1} where $vK = -f$. Let h_2 be the depth at which the subsurface front is defined, 200 m, and let h_s be the depth at which the surface front is defined. If there is no mixed layer, h_s is zero. However, more realistically there will be a mixed layer, and it may be more correct to set h_s equal to the average value of h in the mixed-layer or one-half the mixed layer depth. The separation S between the surface and subsurface fronts is

$$S=x(h_2)-x(h_s). \tag{6}$$

Using Eq. (5) or Fig. 1, S is determined assuming $1/\alpha$ to be 30 km and h_0 to be 660 m. Additionally assuming h_s to be 25 m consistent with a mixed-layer depth of 50 m and h_2 to be 200 m, S is predicted to be 9.7 km when there is zero flow curvature. When the flow curvatures are anticyclonic and cyclonic respectively with 0.015 km^{-1} magnitude, the predicted separations are instead 14.7 and 8.0 km, respectively. Since the average cross-stream slope of h is $(h_2 - h_s)/S$, the average slopes for the anticyclonic, zero, and cyclonic curvatures are respectively 1.2×10^{-2}, 1.8×10^{-2} and 2.2×10^{-2}.

To show simply how the results depend upon the parameters RD and h_0, we derive an approximate solution for h. Stommel's (1972) perturbational solution to first order in αR is

$$h=h_0\left(1-e^{-\alpha x}-\frac{2e^{-2\alpha x}}{3\alpha R}\right). \tag{7}$$

This solution can be further simplified by expanding the exponentials into Taylor series about $x = x_{ax}$; x_a is the cross-stream position midway between surface and subsurface fronts. After a fair amount of algebra it can be shown that

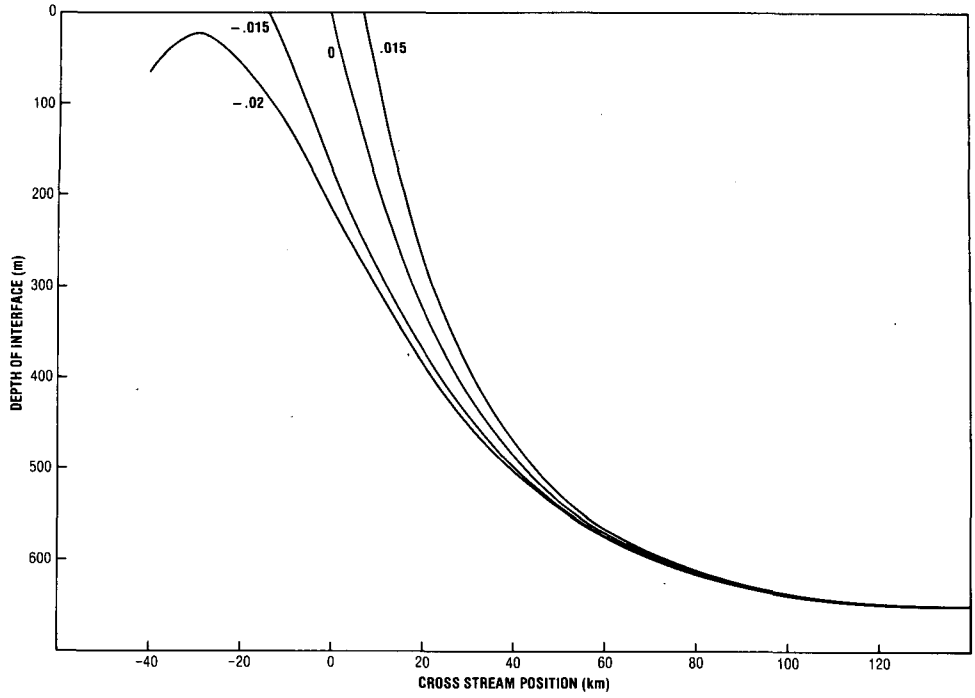

FIG. 1. Depth of interface between upper and lower layers versus cross-system position for several different curvatures. Positive and negative curvatures indicate respectively cyclonic and anticyclonic curvatures.

$$S=\frac{(h_2-h_s)\mathrm{RD}}{h_0 e^{-\alpha x_a}}\left(1-\frac{4K\mathrm{RD}e^{-3\alpha x_a}}{3}\right). \tag{8}$$

Here we have defined RD to be the radius of deformation which is $1/\alpha$. While x_a is not a constant, Eq. 8 shows that the separation for zero curvature is approximately proportional to the radius of deformation RD and inversely proportional to the maximum depth h_0. The strength of the curvature effect $\partial S/\partial K$ is approximately proportional to RD^2. However, if S when $K = 0$ is held constant by varying h_0 or $h_2 - h_s$, the curvature effect is only approximately proportional to RD.

The assumption that the surface and subsurface fronts lie on the interface between the upper and lower layers is equivalent to assuming that they are both on the same isopycnal. Aside from the effects of seasonal heating which greatly modify the near-surface temperatures, this is not true. While the subsurface front is defined as an isotherm–depth pair, the surface front is somewhat loosely defined to be where there is a strong cross-frontal temperature gradient. There can even be more than one surface front. Furthermore, the surface front can be moved in the cross-stream direction relative to the subsurface front by Ekman advection or surface-trapped instabilities. A highly variable surface–subsurface frontal separation is the result.

To permit a variable surface–subsurface frontal separation we allow the surface front to be on an isopycnal different from that which the surface front is on. For this reason, instead of considering the Stream's front to be a discontinuous interface, we now consider the stream's front to be composed of a series of straight and parallel density surfaces. This is a reasonable approximation as shown by Watts' Fig. 9, (1983). Figure 2 shows a schematic of this idealized front with two isopycnals having density difference $\Delta\rho$ and vertical separation Δh. In the figure we assume that the subsurface front lies on the ρ isopycnal at depth h while the surface front is where the $\rho - \Delta\rho$ isopycnal surfaces.

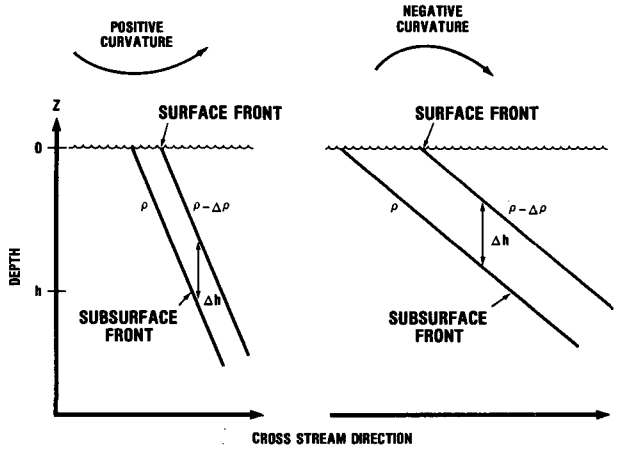

FIG. 2. Cross-stream frontal slope and the normal separation between the isopycnals making up the front. Differences between cyclonic and anticyclonic flow curvature are illustrated.

If the depth of the surface front is not assumed to be zero because of the presence of a mixed layer, then h is the depth difference between the subsurface and surface fronts or $h_2 - h_s$ as defined earlier. Defining s to be the cross-frontal slope of the isopycnals,

$$S = \frac{h - \Delta h}{s}. \tag{9}$$

The slope s is to be inferred from Eq. (5) as the average cross-frontal slope of the interface between the depths h_2 and h_s.

If as in Fig. 2 the surface front is on a less dense isopycnal, then Δh is positive, and S is smaller than if the surface and subsurface were on the same isopycnal. Conversely, if the surface front were on a more dense isopycnal, than Δh would be negative and S would be greater.

The change in separation with curvature is

$$\frac{\partial S}{\partial K} = -\left(S\frac{\partial s}{\partial K} + \frac{\partial \Delta h}{\partial K}\right)\Big/ s. \tag{10}$$

Considering just the first term on the right side of Eq. (10), the strength of the curvature effect is proportional to the frontal separation and the rate of change of frontal slope with curvature. The second term shows that additional changes in frontal separation are induced by a change in the vertical separations between isopycnals. Equation (10) can be simplified by considering the relative importance of the two terms on the right side of (10). To do this $S\partial s/\partial K$ must be compared with $\partial \Delta h/\partial K$.

The rate of change of Δh with K is estimated by requiring, as was done earlier, the conservation of potential vorticity from meander peak to trough. For the continuously stratified case the potential vorticity is

$$\pi = \left(f + \frac{\partial v}{\partial x}\right)\frac{\partial \rho}{\partial z} - \frac{\partial v}{\partial z}\frac{\partial \rho}{\partial x}. \tag{11}$$

The expression for π can be rewritten in the form

$$\pi = \frac{\partial \rho}{\partial z}\left\{f + \frac{\partial v}{\partial x}\left[1 - \left(\frac{\partial x}{\partial z}\right)_v\left(\frac{\partial z}{\partial x}\right)_\rho\right]\right\} \tag{12}$$

where the identities

$$\frac{\partial \rho}{\partial x} = -\frac{\partial \rho}{\partial z}\left(\frac{\partial z}{\partial x}\right)_\rho \tag{13}$$

$$\frac{\partial v}{\partial z} = -\frac{\partial v}{\partial x}\left(\frac{\partial x}{\partial z}\right)_v \tag{14}$$

have been used. As Hoskins and Bretherton (1972) discuss, in the vicinity of very strong fronts where horizontal vorticity and density gradients are very large, the cross-frontal slopes holding v and ρ constant tend to be similar. This keeps the potential vorticity bounded. Indeed, if the two slopes were equal, Eq. (12) shows that π would equal $f\partial\rho/\partial z$. Gulf Stream sections shown by Newton (1978) and Warren and Volkman (1968) allow the cross-stream slopes holding current speed and temperature constant to be compared. Comparing the slopes on the cyclonic sides of the currents where the isotherms have steep slopes, the cross-stream slopes holding current speed are generally about 50% greater than the slopes holding temperature or effectively, density constant. Therefore, assuming $(\partial z/\partial x)_v$ to be 50% greater than $(\partial z/\partial x)_\rho$,

$$\pi \approx \frac{\partial \rho}{\partial z}\left(f + \tfrac{1}{3}\partial v/\partial x\right). \tag{15}$$

In natural coordinates

$$\frac{\partial v}{\partial x} = \frac{\partial v}{\partial n} + vK \tag{16}$$

where n is the direction to the right of the flow direction. Using $f' = f + \frac{1}{3}\partial v/\partial n$ and $\Delta\rho/\Delta h = \partial\rho/\partial z$,

$$\pi \approx \frac{\Delta \rho}{\Delta h}(f' + vK/3). \tag{17}$$

Assuming v to be 80 cm s^{-1} and f' to be 10^{-4} s^{-1}, we estimate $\partial \Delta h/\partial K$. If K varies from 0.015 to -0.015 km^{-1}, from trough to peak, $f' + \frac{1}{3}vK$ undergoes a fractional change of about 8%. This fractional change must be compensated by an equivalent fractional change in Δh if potential vorticity is conserved from peak to trough. Therefore, for the curvatures used the vertical separation Δh between isopycnals will be about 4% greater (smaller) at the meander trough (peaks) than where the curvature is zero. In comparison, it can be inferred from Eq. (5) or Fig. 1 that for the same circumstances the cross-frontal slope s which is $(\partial z/\partial x)_\rho$ undergoes a fractional change of about 50% from trough to peak. The constancy of Δh and hence $\partial\rho/\partial z$ relative to $(\partial z/\partial x)_\rho$ means that the magnitude of $\partial\rho/\partial x$ will decrease from trough to peak. These conclusions are supported by Newton (1978). He shows a temperature section across the Gulf Stream where the curvature was cyclonic along with a nearby section where the curvature was anticyclonic. The two sections show a dramatic difference in the cross-stream slopes of the isotherms as well as their horizontal separations. Yet, between the two sections there is no obvious change in the isotherms vertical separations. As will be discussed, the cross-stream movement of the isopycnals as they unpack or pack in response to changes in K modifies changes in frontal separations due solely to changes in the cross-frontal slope s.

The relative importance of $S\partial s/\partial K$ and $\partial \Delta h/\partial K$ in Eq. (10) can now be compared. Consistent with observations to be shown we choose S to be 20 km when K is zero. The slope s when K is zero is assumed to be the average $\partial h/\partial x$ over the depth range from 25 to 200 m inferred from Eq. (5). The value for s is 1.8×10^{-2}. Using Eq. (9), the appropriate Δh is -177 m. Finally,

using our estimate that s varies by 50% while Δh varies by only 8% as K changes from 0.015 km^{-1} to -0.015^{-1},

$$\left.\begin{aligned} S\frac{\partial s}{\partial K} &= 6 \text{ km}^2 \\ \frac{\partial \Delta h}{\partial K} &= -0.5 \text{ km}^2 \end{aligned}\right\}.$$

For these parameters $\partial\Delta h/\partial K$ is unimportant relative to $S\partial s/\partial K$ and it is a reasonable approximation that

$$\frac{\partial S}{\partial K} = -\left(S\frac{\partial s}{\partial K}\right)\Big/ s. \tag{18}$$

Equation (18) is a good approximation for the RD, h and h_0 chosen unless S is smaller than a few kilometers. For example, if S is 10 km then Δh is nearly zero, and the approximation is almost perfect. If S is 5 km, Δh is 89 m, and $\partial\Delta h/\partial K$ is 20% as large as $S\partial s/\partial K$. If S is zero, Eq. (18) is still a usable approximation. Using the same parameters we estimate from Eq. (10) that $\partial S/\partial K$ is only about 30 km^2 if S is zero. This corresponds to a change in S of about 1 km in response to a change in K of 0.03 km^{-1}. A response of this magnitude can not be reliably observed.

The primary result of Eq. (18) is that the strength of the curvature effect is proportional to surface–subsurface frontal separation. This dependence of $\partial S/\partial K$ upon S is easy to understand if the changes in horizontal separation between isopycnals are considered. If the cross-stream frontal slope increases due to cyclonic flow, the packing of the isopycnals moves a lighter isopycnal to the left (looking downstream) relative to a denser isopycnal. Conversely, if the flow curvature is anticyclonic, the unpacking of the isopycnals moves a lighter isopycnal to the right relative to a denser isopycnal. The net result is that the curvature effect is enhanced(diminished) if the isopycnal defining the position of the surface front is more(less) dense than the isopycnal defining the subsurface front. This is why the curvature effect is proportional to the separation between the surface and subsurface fronts. Hence, the curvature effect should be most obvious when the separation is greater than its historical average and should be nonexistent when the separation is zero. Of course, if the separation is too different from its historical mean, the surface front will no longer be over the stream's subsurface front and the assumptions of the derivation will not be valid.

Figure 3 illustrates the dependence of the strength curvature effect upon separation. The path of a meandering subsurface front along with two surface fronts is shown in the figure. The meander in the subsurface front has an amplitude of 30 km and a wavelength of 300 km. The separations between the surface and subsurface fronts for zero subsurface front curvature are 10 and 30 km. Changes in separation due to flow curvature were computed assuming as in the earlier examples, an internal radius of deformation RD of 30 km. In making the calculation, h_2 and h_s were chosen to be 200 and 25 m, respectively, so that h in Eq. (10) is 175 m. The slope s in Eq. (18) was computed as a function of K using Eq. (5) assuming it to be the average $\partial h/\partial x$ between h_s and h_2. Finally, the depth differences Δh were chosen so that the separations for zero curvature were correct. This allowed the surface–subsurface frontal separation to be computed a a function of curvature. Instead of considering the two lines in Fig. 3 to be separate surface fronts, they may instead be viewed as separate isotherms composing a single surface front. The interpretation of the figure then is that the width of the surface front is curvature dependent.

4. Observations

Using surveyed frontal paths (Horton, 1984a) we computed frontal separations and subsurface front

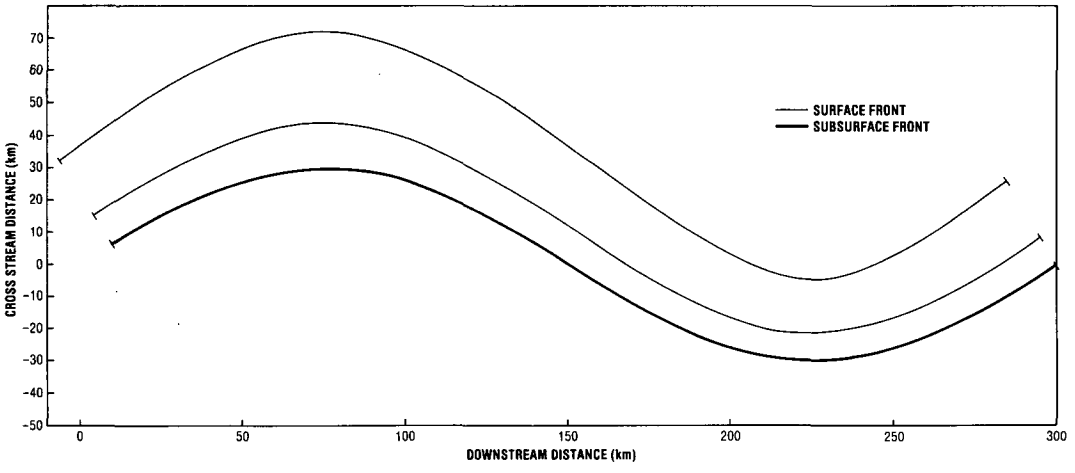

FIG. 3. Surface fronts with surface–subsurface frontal separations, where the curvature of the subsurface front is zero, of 10 and 30 km. The surface fronts may instead be viewed as the two isotherms forming the boundary of a single surface front.

curvatures where possible. The major problem was that the surface front was strongly contaminated with surface-trapped eddies or folded-wave features. These features strongly modify frontal separation especially where they lead to flow reversals in the surface front. Comparisons between front separation and subsurface front curvature were not made where the surface front was apparently contaminated. While comparisons between frontal separation and subsurface path were poorly tracked, an effort was made to get as many comparisons as possible. These computations are illustrated in Fig. 4, where we plot separation against subsurface front curvature. Since Hurricane Dennis affected the separation distance so greatly, the data is partitioned into before-and-after hurricane sets. Also, the linear least-square fit of separation distance against subsurface front curvature is included for each dataset.

Before the passage of Dennis the slope of the regression line was -418 km^2 with a single standard deviation uncertainty of 199 km^2 based upon 32 measurements of separation versus curvature. However, the apparently significant slope of the regression line was due to just a few of the measurements. West of 70°W the surface front was generally to the north of the subsurface front, while to the east of 70°W the surface front was often to the south of the subsurface front. The regression line was again computed using just the 26 measurements east of 70°W. For this case the separation between the surface and subsurface fronts for zero curvature was approximately zero. The new slope of the regression line was -164 km^2 with a standard deviation of 195 km^2. Thus, we see that where the separation for zero curvature was essentially zero, the slope of the regression line was not significant. This is consistent with Eq. (18), which says that there is no curvature effect when the separation between the surface and subsurface fronts is zero.

After the passage of Dennis the slope of the regression line was -424 km^2 with a standard deviation of 92 km^2. The separation for zero curvature was 18.6 km. Because the predicted solution of separation S versus curvature K from Eqs. (9) and (5) is approximately exponential, an exponential regression curvature was also filled to the post-storm observations of Fig. 4. For this curve the separation for zero curvature is 16.2 km. However, the linear and exponential curves are quite similar, and the data is probably to noisy to distinguish between them.

Figure 5 plots versus K the strength of the curvature effect, $\partial S/\partial K$, given by the fit of the exponential curve to the post-storm observations of Fig. 4. The error bars are the estimated 95% confidence limits. In order to compare theoretical predications with observations, $\partial S/\partial K$ was computed from Eq. (18) using Eq. (5) to determine the cross-frontal slope s. In making his calculation RD was assumed to be 30 km and h_s was chosen to be 25 m consistent with the observed mixed-layer depth of 50 m. In order that S in Eq. (18) be the observed 17.2 km when K is zero, Δh was chosen to be -114 m. Predictions and observations agreed within or almost within the error bars for curvatures between -0.012 and 0.0175 km^{-1}. Averaged over curvatures between ± 0.01 km^{-1}, the modeled $\partial S/\partial K$ agreed within 5% of the observed $\partial S/\partial K$. The modeled magnitude of

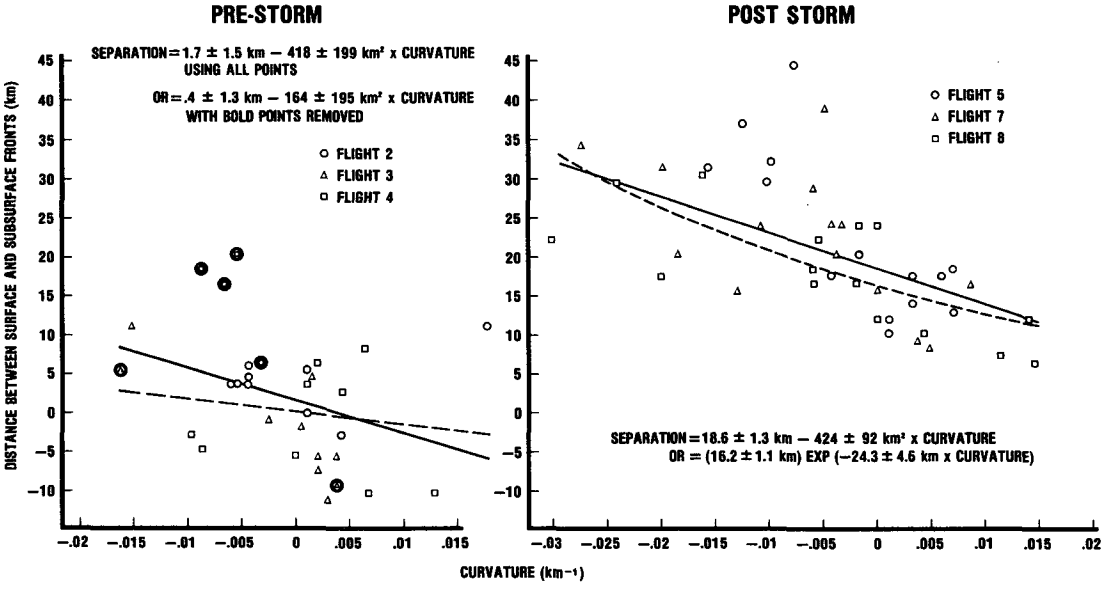

FIG. 4. Observed surface-subsurface frontal separations plotted against subsurface front curvature. Observations taken before Hurricane Dennis are plotted separately from those taken after. For the before-Dennis set, the regression line was also computed using the reduced set of observations described in the text.

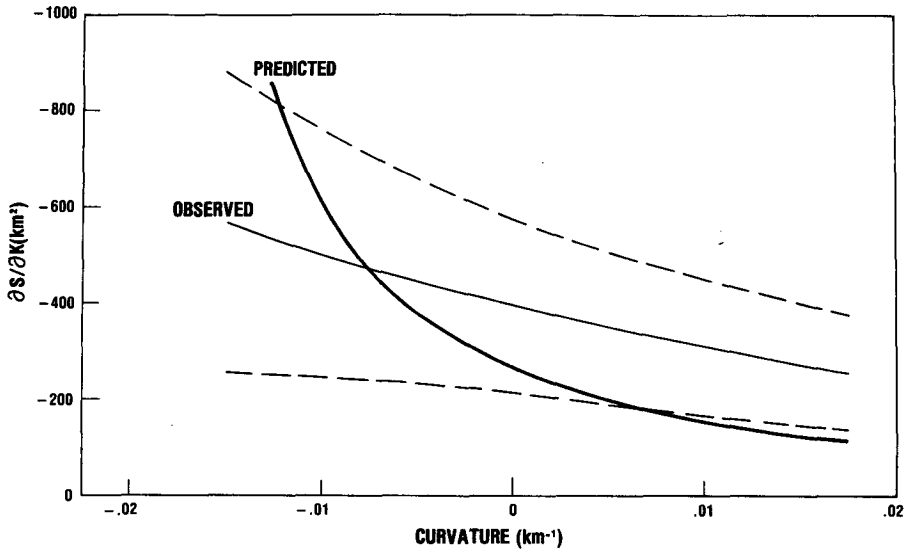

FIG. 5. Predicted strength of curvature effect $\partial S/\partial K$ for the post-storm case computed using Eq. (18), compared with $\partial S/\partial K$ obtained from the exponential regression line fitted to the post-storm observations of Fig. 4.

$\partial S/\partial K$ is approximately proportional to RD. Because RD is observed to vary by almost a factor of two between the slope water and Sargasso water, RD could reasonably be changed to improve the comparison.

The modeled $\partial S/\partial K$ becomes less certain with increasing curvature because the use of natural coordinates by Eq. (2). The use of natural coordinates assumes that the path curvature remains small so that the radius of curvature remains much greater than the width of the stream. Consequently model predictions become unreliable for curvatures exceeding approximately ± 0.01 km^{-1}. The very large modeled $\partial S/\partial K$ for curvatures less than -0.01 km^{-1} are especially suspect, and the increasing difference there between model predictions and observations in Fig. 5 are probably due to a failure of the model.

Additional support for Eq. (18) is provided by the observations of Horton (1984b). During these observations the mean surface–surface separation was relatively small 4 km. In qualitative agreement with Eq. (18), inspection of these observations showed no strong or obvious correlation between surface–subsurface frontal separation and subsurface front path curvature.

5. Conclusion

An analytical relationship has been obtained which describes the modulation of the surface–subsurface frontal separation by the path curvature of the subsurface front. The strength of the modulation is predicted to be proportional to the surface–subsurface frontal separation. Because, for other reasons, the frontal separation is quite variable, there may or may not be significant modulation of the frontal separation by path curvature. The theory was shown to be in reasonable agreement with observations taken by Horton (1984a,b). In these observations the modulation the surface–subsurface frontal separation was only reliably seen when the frontal separation was relatively large and averaged about 19 km. For this case predictions were generally within the error bounds of the observations when the radius of deformation was assumed to be 30 km. Because the radius of deformation changes from about 25 km in slope water to 40 km in Sargasso water, the comparison could have been improved by using a different but still reasonable radius of deformation.

Given the Gulf Stream surface–subsurface frontal separation and path curvature at some point, this model in principle allows downstream changes in frontal separation to be predicted. Operationally this might be done by combining satellite infrared observations of the Gulf Stream surface front with subsurface frontal positions inferred from satellite altimetry or from surface drifters with thermister strings. A practical consideration, though, is that changes in frontal separation due to other processes, such as surface-trapped meanders, might dominate the curvature effect.

REFERENCES

Bane, J. M., D. A. Brooks and K. R. Robinson, 1981: Synoptic Observation of the three-dimensional structure and propagation of Gulf Stream meanders along the Carolina Continental Margin. *J. Geophys. Res.*, **86**, 6411–6455.

Chew, F., 1974: The turning process in meandering currents: A case study. *J. Phys. Oceanogr.*, **4**, 27–54.

Fuglister, F. C., and L. V. Worthington, 1951: Some results of a multiple ship survey of the Gulf Stream. *Tellus*, **3**, 1–14.

Hansen, D. V., and G. Maul, 1970: A note on the use of sea-surface temperature for observing ocean currents. *Remote Sensing of the Environment.* **1**, 161–164.

Horton, C. W., 1984a: Surface front displacement in the Gulf Stream by Hurricane/Tropical Storm Dennis. *J. Geophys. Res.*, **89,** 2005–2017.

——, 1984b: Observations of a near-surface Gulf Stream eddy and of changes in the surface–subsurface frontal separation. *J. Phys. Oceanogr.*, **14,** 1407–1413.

Hoskins, B. J., and F. P. Bretherton, 1972: Atmospheric frontogenesis models. Mathematical formulation and solution. *J. Atmos. Sci.*, **29,** 11–37.

Maul, G. A., 1975: An evaluation of the use of earth resource technology satellite for observing ocean current boundaries in the Gulf Stream system. *ERL 335-AOML,* **8,** NOAA, Boulder.

Newton, C. W., 1978: Fronts and wave disturbances in Gulf Stream and atmospheric jet stream. *J. Geophys. Res.*, **83,** 4697–4706.

Robinson, A. R., R. Luyten and F. L. Fuglister, 1974: Transient Gulf Stream meandering. Part I: An observational experiment. *J. Phys. Oceanogr.*, **4,** 237–302.

Rossby, T., A. S. Bower and P-T. Shaw, 1985: Particle pathways in the Gulf Stream. *Bull. Amer. Meteor. Soc.*, **66,** 1106–1110.

Stommel, H., 1972: *The Gulf Stream,* University of California Press, Los Angeles, CA.

Warren, B. A., and G. H. Volkmann, 1968: Measurement of volume transport of the Gulf Stream south of New England. *J. Mar Res.*, **26,** 110–126.

Watts, D. R., 1983: Gulf Stream variability. *Eddies in Marine Science,* A. R. Robinson, Ed., Springer-Verlag, 114–144.

Webster, F., 1961: A description of Gulf Stream meanders off Onslow Bay. *Deep-Sea Res.*, 130–143.